

MIXED-MODE DELAMINATION FRACTURE TOUGHNESS OF UNIDIRECTIONAL GLASS/EPOXY COMPOSITES UNDER FATIGUE LOADING

M. Kenane & M. L. Benzeggagh

Université de Technologie de Compiègne, Laboratoire de Génie Mécanique, Polymères et Composites, LG2ms URA CNRS 1505, BP 529, 60205 Compiègne Cedex, France

(Received 2 August 1996; revised 18 November 1996; accepted 13 December 1996)

Abstract

Delamination fatigue-crack growth experiments have been carried out on unidirectional glass/epoxy laminates. Three specimen types were tested: double cantilever beam (DCB), mixed-mode bending (MMB), and end-loaded split (ELS), for mode I, mixed-mode I + II, and mode II loading, respectively. Fracture mechanics technology was applied through the principles of strain-energy release rate. The measured delamination growth rates, da/dN , were correlated with the corresponding strain-energy release rates, ΔG_I , ΔG_T , and ΔG_{II} . A large number of G_{II}/G_T mode ratios has been used in order to cover the maximum number of cases in the range from 0 to 100%.

A semi-empirical fatigue criterion is proposed. Experimental results are correlated with this criterion through the plot of parameters d and B versus the G_{II}/G_T mode ratio. The predicted behaviour is in good agreement with experimental results. © 1997 Elsevier Science Limited

Keywords: glass/epoxy, mode I, mode II, mixed mode, strain-energy release rates, fatigue, crack growth rate, empirical criterion

NOTATION

B	Coefficient in fatigue-crack growth law
C	Compliance
d	Exponent in fatigue-crack growth law
da/dN	Fatigue-crack growth rate
DCB	Double cantilever beam
ELS	End-loaded split
ΔG	Strain-energy release rate range
G_{IC}, G_{IIC}, G_{TC}	Mode I, mode II and total critical strain-energy release rate
MMB	Mixed-mode bending
n and h	Constants in mode I compliance
R	Cyclic load ratio

α and β Constants in mixed-mode and mode II compliances

1 INTRODUCTION

The interlaminar damage mechanism is the most severe type of defect since it may significantly reduce the stiffness and strength of a material. Thus, it is a critical damaging mechanism that should be carefully considered in the evaluation of laminated composite structures for durability and damage tolerance. It results generally from mode I, mode II or mixed mode I + II loading.

Crack propagation under pure mode I (opening mode) and pure mode II (shearing mode) cyclic loading has been extensively studied in the literature, but more attention must be paid to mixed mode I + II loading because it relates to most realistic situations. In fact, composite structures are generally subjected to combinations of mode I and mode II.

Concerning the mixed mode, different configurations for a test specimen have been proposed, but most of them present practical limitations. The mixed-mode bending (MMB) test, proposed by Crews and Reeder,¹ seems to be very interesting. It has been adapted to our material by Aboura *et al.*² from the work of Reeder *et al.*³ works. The MMB test presents some advantages, including the possibility of working with a wide range of mixed-mode ratios with the same specimen geometry. The G_{II}/G_T mode ratio was also found to be independent of the crack length.

In a previous study⁴ of monotonic tests, it was found that the semi-empirical criterion proposed by Gong and Benzeggagh⁵ predicts the total critical strain-energy release rate, G_{TC} , and the total fracture energy, G_{TR} , under any combination of modes I and II:

$$G_{TC} = G_{IC} + (G_{IIC} - G_{IC}) \left(\frac{G_{II}}{G_T} \right)^m$$

where m is a characteristic parameter of the material considered.

The delamination crack growth rate, da/dN , may be related to the strain-energy release rate, ΔG ,^{6,7} by a relationship of the form:

$$\frac{da}{dN} = B(\Delta G)^d$$

Thus, for each value of the mode ratio G_{II}/G_I there are corresponding values of d and B .

In this work, we have used the MMB test to investigate the mixed-mode I + II crack-propagation behaviour in interlaminar fatigue tests. Experimental results are used to predict delamination growth rate through the Paris power law.

2 MATERIAL AND SPECIMEN

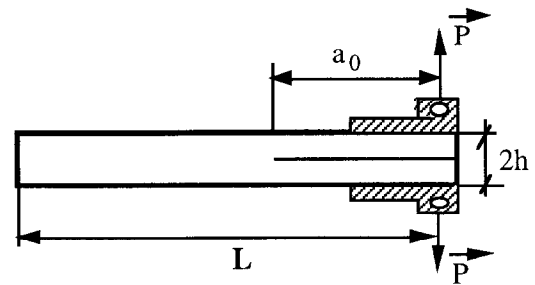
The laminates tested in this work were made by compression moulding of 16 quasi-unidirectional plies of prepreg of 52 vol% of E-glass fibre with M10 epoxy resin (VICOTEX), which were stacked in a sheet 6 mm thick. Five percent of fibres were woven perpendicularly to hold the parallel fibres together and they could set a limit to the crack shifting. The starter crack was formed by inserting a 0.06 mm thick PTFE film at mid-thickness during manufacture.

The elastic constants were determined from panels produced from the same prepreg,⁸ and are given in Table 1.

The pure mode I values for interlaminar fracture toughness, G_I , are usually obtained by using a double cantilever beam (DCB) (Fig. 1). The pure mode II delamination test specimen used in this study is the end-loaded split (ELS) specimen (Fig. 2). The mixed-mode fracture tests were conducted by means of the MMB method, which is a simple combination of the DCB (mode I) specimen and the ENF (mode II) specimen (Fig. 3).

3 EXPERIMENTAL

The experiments were carried out in a 1 kN, computer-controlled, servo-hydraulic testing machine (Instron 1341). Fatigue-induced delamination growth was characterised by conducting constant-amplitude fatigue tests at a minimum to maximum cyclic load ratio (R) of 0.1 and a frequency of 4 Hz. During tests,



$$L = 150 \text{ mm} \quad B = 20 \text{ mm}$$

$$2h = 6 \text{ mm}$$

Fig. 1. DCB specimen.

the maximum and the minimum strain-energy release rates, G_{\max} and G_{\min} , and the delamination growth rate, da/dN , were monitored.

4 MIXED-MODE BENDING TEST

The mode I and mode II components, P_I and P_{II} , respectively, are given by the following equations:

$$P_I = \frac{3e - L}{4L} P \quad (1)$$

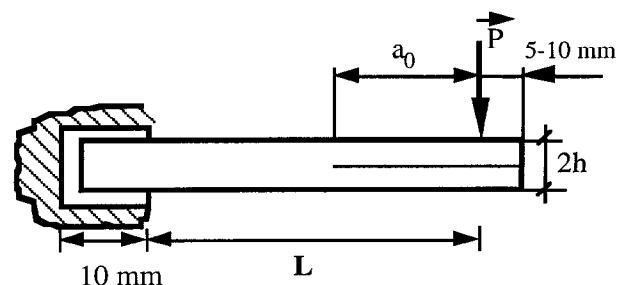
$$P_{II} = \frac{e + L}{L} P \quad (2)$$

Figure 4 illustrates the superposition of mode I and mode II components in the MMB rig.^{1,3}

According to Reeder and Crews,⁹ the mode I and mode II components of G are given by the following equations:

$$G_I = \frac{4P(3e - L)^2}{64bL^2E_{11}I} \left(a^2 + \frac{2a}{\lambda} + \frac{1}{\lambda^2} + \frac{h^2E_{11}}{10G_{12}} \right) \quad (3)$$

$$G_{II} = \frac{3P^2(e + L)^2}{64bL^2E_{11}I} \left(a^2 + \frac{h^2E_{11}}{5G_{12}} \right) \quad (4)$$



$$L = 65 \text{ mm} \quad B = 20 \text{ mm}$$

$$2h = 6 \text{ mm}$$

Fig. 2. ELS specimen.

Table 1. Elastic constants for E-glass/M10-epoxy composite

$E_{11} = 36.2 \text{ GPa}$	$G_{12} = 5.6 \text{ GPa}$	$\nu_{12} = 0.26$
$E_{22} = 10.6 \text{ GPa}$	$G_{13} = 3.7 \text{ GPa}$	$\nu_{13} = 0.33$
$E_{33} = 7.2 \text{ GPa}$	$G_{23} = 3.2 \text{ GPa}$	$\nu_{23} = 0.48$

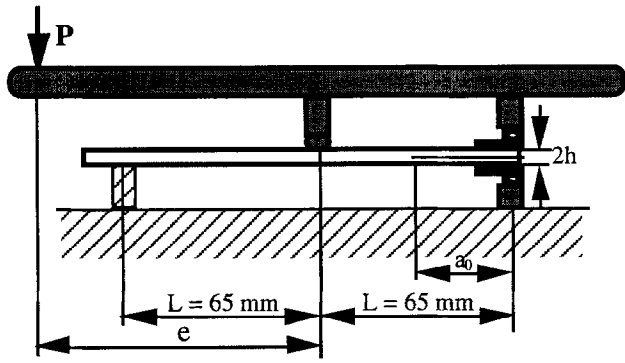


Fig. 3. MMB specimen.

response to calibrate experimentally the compliance law, $C = F(a)$. From the linear analysis, the experimental compliance laws for the MMB and ELS tests used in this study were expressed as:

$$C = \alpha + \beta a^3$$

where the material constants α and β were dependent on the mixed-mode ratio. The values of α and β , which were determined by interpolating the measured compliances, are presented in Table 2.

The critical strain-energy release rates, G_{IC} and G_{IIC} , from mode I and mode II tests, respectively, and the total critical strain-energy release rate, G_{TC} , from different mixed modes considered in this work can be calculated⁴ and results are given in Table 3.

5 RESULTS AND DISCUSSION

In general, for all modes considered in this study, the measured delamination growth rate data obey a power-law relationship of the form:

$$\frac{da}{dN} = B(\Delta G)^d \tag{8}$$

where $\Delta G = G_{max} - G_{min}$ and B and d are constants depending on the material, temperature, stress ratio, R , and frequency.^{10,11} G_{max} corresponds to P_{max} and G_{min} corresponds to P_{min} .

As can be seen from Fig. 5, for all the G_{II}/G_T ratios considered, the crack-growth rate increases progressively from $a = 35$ mm to $a = 40$ mm, beyond which the increase is more marked. Concerning the propagation, we note that is relatively unstable for high mode ratios but is stable for low mode ratios. This is particularly true in the monotonic case where the propagation in pure mode II is characterised by a marked instability, by contrast with pure mode I where the propagation is stable.

The measured crack growth rate data are correlated with the corresponding strain-energy release rate for each over G_{II}/G_T mode ratio, pure mode I and pure mode II, as shown in Figs 6–13, and the results may be fitted by eqn (8). The coefficients B and d , obtained by least-squares fitting of the fatigue-crack growth rate curves, are also presented in these figures.

where

$$I = \frac{bh^3}{12} \quad \text{and} \quad \lambda = \frac{1}{h} \sqrt[4]{\frac{6E_{22}}{E_{11}}}$$

From eqns (3) and (4), we obtain the mode ratio, G_{II}/G_T :

$$\frac{G_{II}}{G_T} = \frac{3(e+L)^2}{3(e+L)^2 + 4(3e-L)^2} \tag{6}$$

We note that G_{II}/G_T is independent of the crack length, a .

4.1 Energy release rates

For linear-elastic material behaviour, the energy release rate, G , was calculated from the following expression:

$$G = \frac{P^2 dC}{2b da} \tag{7}$$

where b is the width of the specimen (mm), P is the applied load (N) and C is the compliance ($N\text{ mm}^{-1}$).

The mode I compliance from the DCB specimen is given empirically by the relationship

$$C = \frac{a^n}{h}$$

where n and h are empirical laminate parameters found from the measured compliance to be $n = 1.89$, $h = 24.78 \times 10^5$.

For a given mixed mode, the compliances of the load point, $C = \delta/P$, for different initial crack lengths, a , were measured from the load/displacement

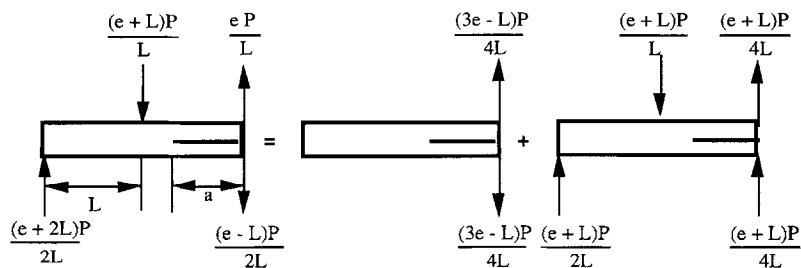


Fig. 4. Decomposition and analysis of the MMB specimen by beam theory.

Table 2. Constants for compliance fits

	G_{II}/G_T (%)						Mode II
	28	43	53	72	82	91	
α ($10^{-3} \text{ mm N}^{-1}$)	33.86	20.74	15.38	12.41	11.48	8.94	1.85
β ($10^7 \text{ N}^{-1} \text{ mm}^{-2}$)	3.52	1.47	1.11	0.75	1.05	0.99	1.06

Table 3. Strain-energy release rate values

	G_{II}/G_T (%)							
	0 (mode I)	28	43	53	72	82	91	100 (mode II)
G_{TC} (J m^{-2})	118.02 (2.75)	340.35 (37.26)	568.36 (98.58)	579.62 (58.66)	1033.67 (174.11)	1821.93 (84.47)	2457.76 (100.10)	2905.76 (224.55)

We note that we have not determined the fatigue threshold, ΔG_{TH} .

In most of the studies recorded in the literature, researchers have used graphite/epoxy as the experimental material,¹²⁻¹⁴ so that it is difficult to compare our results. Nevertheless, we note that the d exponent for graphite/epoxy composites is generally much higher than that for glass/epoxy composites (Table 4). In fact, Mall *et al.*¹² studied three

graphite/epoxy composites with different matrix toughness values, and in both mode I and mode II their d values were higher than those obtained in our study. Prel *et al.*¹³ give a d value of 1.6 for glass/epoxy tested in mode I, which is considered to be close to what we have obtained. Other results in the literature give a value of 3.71 for mode I and 7.61 for mode II in the case of a glass-cloth-reinforced epoxy under similar loading conditions.¹⁵ In this case a crack can be

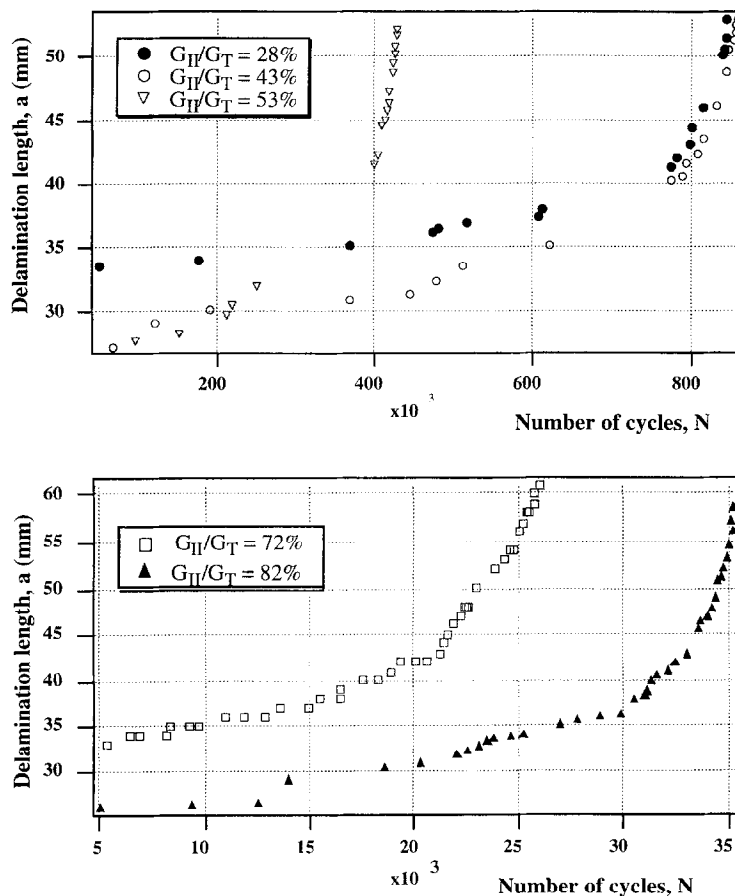


Fig. 5. Representative plots of crack length versus number of cycles.

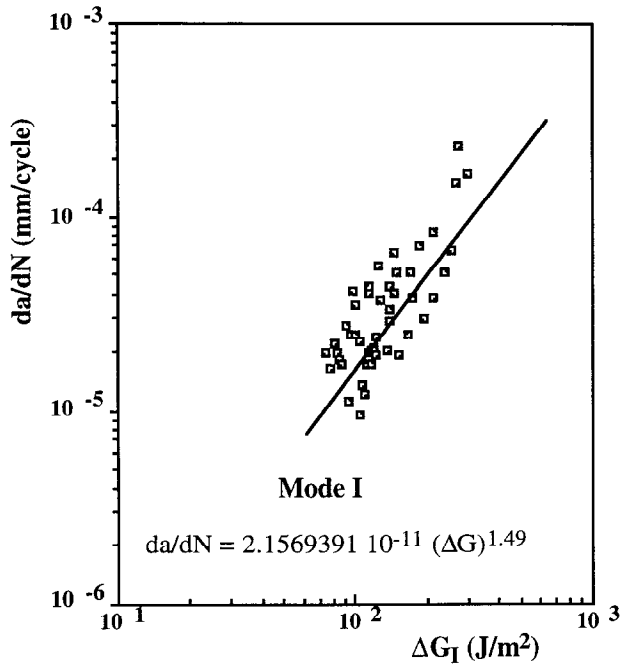


Fig. 6. Delamination growth rate, da/dN , versus the strain-energy release rate, ΔG_I , for mode I.

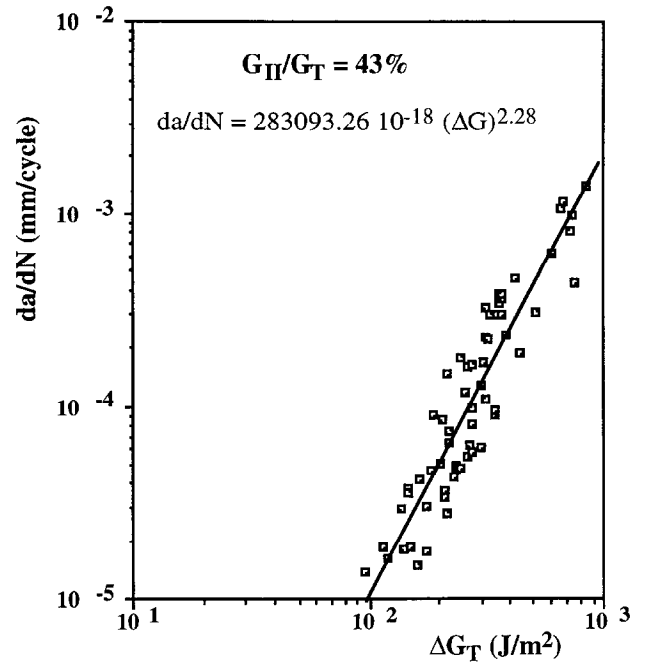


Fig. 8. Delamination growth rate, da/dN , versus the strain-energy release rate, ΔG_T , for $G_{II}/G_T = 43\%$.

confronted locally with several rigidities, unlike in a unidirectional composite where the crack propagates in the plane in which the rigidity is relatively homogeneous.^{16,17}

Concerning the mixed mode, the literature results for graphite/epoxy show that the d exponent decreases with the G_{II}/G_T ratio. However, for

glass/epoxy, results obtained in this study show that the d exponent increases with G_{II}/G_T .

5.1 Empirical mixed-mode fatigue criterion

By contrast with mixed-mode monotonic behaviour, few criteria for mixed-mode fatigue have been proposed. Ramkumar and Whitcomb¹⁸ were the first

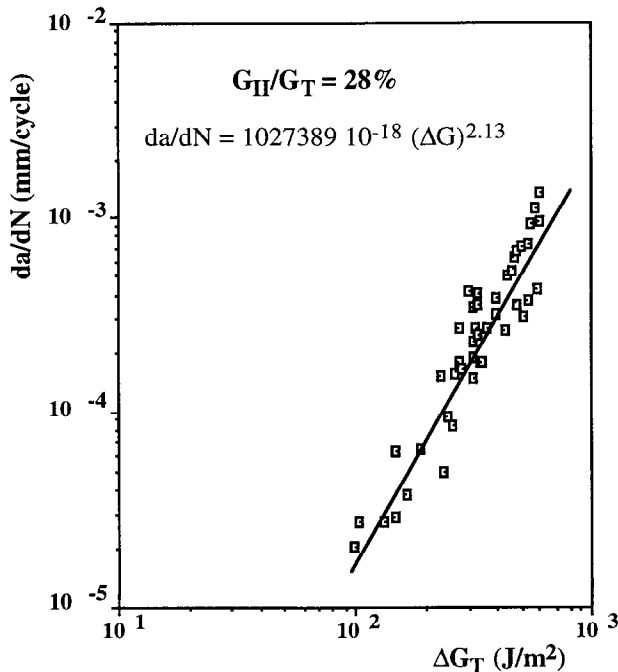


Fig. 7. Delamination growth rate, da/dN , versus the strain-energy release rate, ΔG_T , for $G_{II}/G_T = 28\%$.

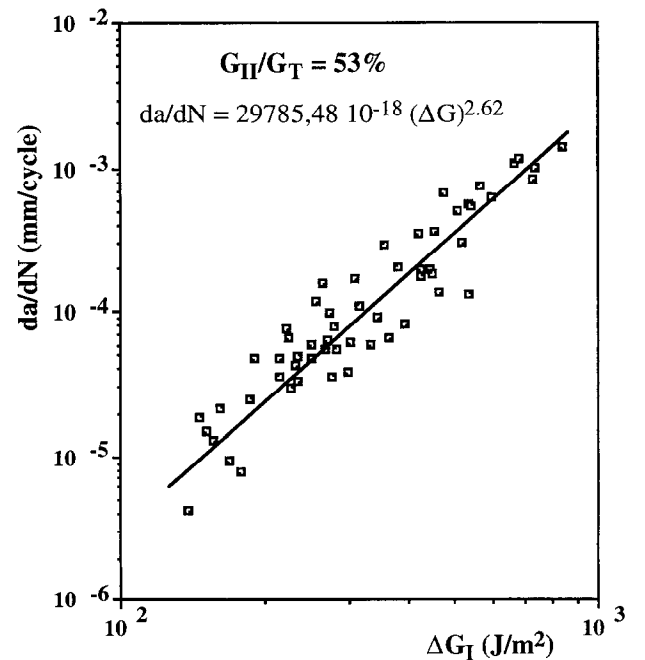


Fig. 9. Delamination growth rate, da/dN , versus the strain-energy release rate, ΔG_T , for $G_{II}/G_T = 53\%$.

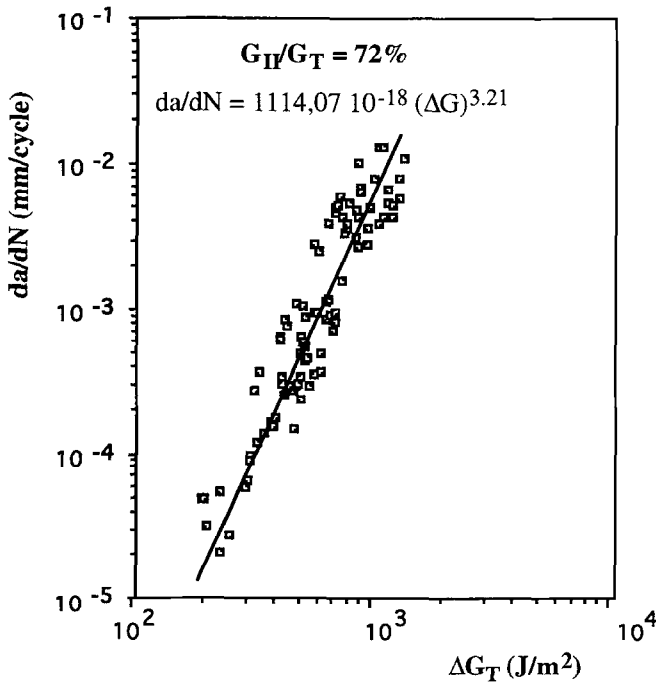


Fig. 10. Delamination growth rate, da/dN , versus the strain-energy release rate, ΔG_T , for $G_{II}/G_T = 72\%$.

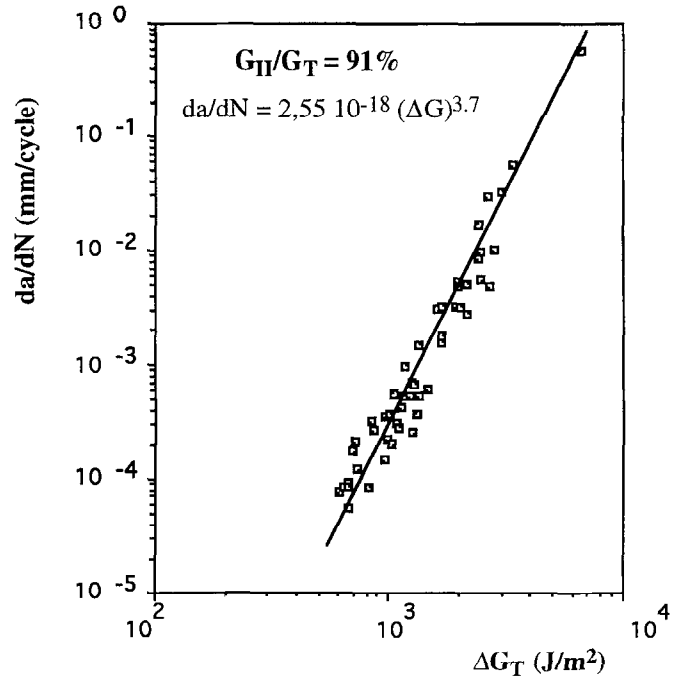


Fig. 12. Delamination growth rate, da/dN , versus the strain-energy release rate, ΔG_T , for $G_{II}/G_T = 91\%$.

to propose a mixed-mode fatigue criterion, followed by Gustafson and Hojo¹⁹ and Russel and Street.²⁰ Recently, Dahlen and Springer²¹ have proposed a more complete criterion taking account the material properties, the loading conditions, the stress ratio, and the mode ratio.

Nevertheless, to have good precision of results

predicted by any criterion, it is necessary to include several G_{II}/G_T ratios in the study in order to cover the maximum number of cases in the range from 0 to 100%. In our case, we propose a semi-empirical criterion for predicting the d and B values of the relationship $da/dN = B(\Delta G)d$ for any G_{II}/G_T mode ratio considered. The relationship for d as a function

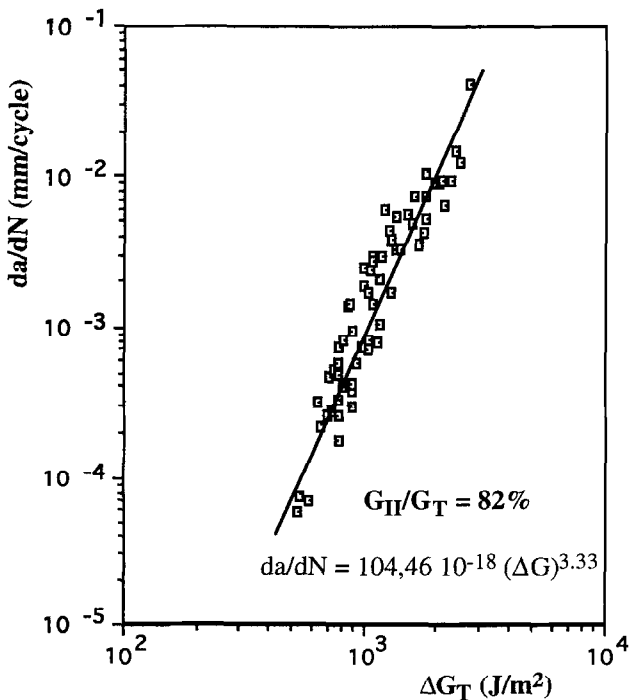


Fig. 11. Delamination growth rate, da/dN , versus the strain-energy release rate, ΔG_T , for $G_{II}/G_T = 82\%$.

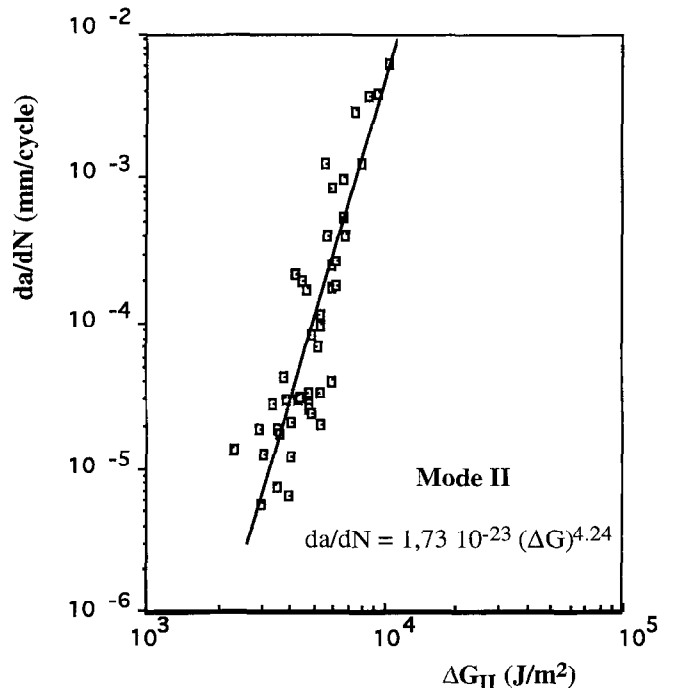


Fig. 13. Delamination growth rate, da/dN , versus the strain-energy release rate, ΔG_{II} , for mode II.

Table 4. Results published in the literature

	Ref.	Mode I		Mode II	
		d	B	d	B
T300/3100	12	7.03	3.68×10^{-19}	5.8	3.29×10^{-18}
IM6/R6376	12	6.4	1.64×10^{-19}	4.62	6.12×10^{-15}
AS4/APC-2	12	4.8	1.8×10^{-17}	3.66	9.11×10^{-13}
AS4/PEEK (1)	13	10.5	—	—	—
AS4/PEEK (2)	14	6.14	—	3.645	—
E-Glass/epoxy M10	13	1.6	—	2.8	—
E-Glass/epoxy 914	15	3.71	3.4×10^{-15}	7.61	1.23×10^{-28}
E-Glass/epoxy M10	This study	1.49	2.16×10^{-11}	4.24	1.71×10^{-23}

of G_{II}/G_T takes the form:

$$d = \alpha_0 + \alpha_1 \left(\frac{G_{II}}{G_T} \right)^{m_d}$$

In pure mode I:

$$\frac{G_{II}}{G_T} = 0 \quad \text{and} \quad d = d_I \Rightarrow \alpha_0 = d_I$$

In pure mode II:

$$\frac{G_{II}}{G_T} = 1 \quad \text{and} \quad d = d_{II} \Rightarrow \alpha_0 = d_{II} - d_I$$

Thus

$$d = d_I + (d_{II} - d_I) \left(\frac{G_{II}}{G_T} \right)^{m_d}$$

For the coefficient B , it is possible to formulate the relationship

$$\ln(B) = \ln(B_{II}) + [\ln(B_I) - \ln(B_{II})] \left(1 - \frac{G_{II}}{G_T} \right)^{m_B}$$

In pure mode I:

$$\frac{G_{II}}{G_T} = 0 \Rightarrow B = B_I$$

In pure mode II:

$$\frac{G_{II}}{G_T} = 1 \Rightarrow B = B_{II}$$

The experimental measurements of d and B have been plotted as a function of G_{II}/G_T in Figs 14 and 15. The proposed criterion gives good results for $m_d = 1.85$ and $m_B = 0.35$. It seems able to describe mixed-mode interaction under cyclic loading:

$$d = 1.885 + 2.255 \left(\frac{G_{II}}{G_T} \right)^{1.85}$$

$$\ln(B) = -52.616 - 28.058 \left(1 - \frac{G_{II}}{G_T} \right)^{0.35}$$

Table 5 presents a comparison between results from experiment and by using the criterion. Nevertheless, in order to verify the validity of the d and B relationships, it would be interesting to study composites with several different matrices and interfaces.

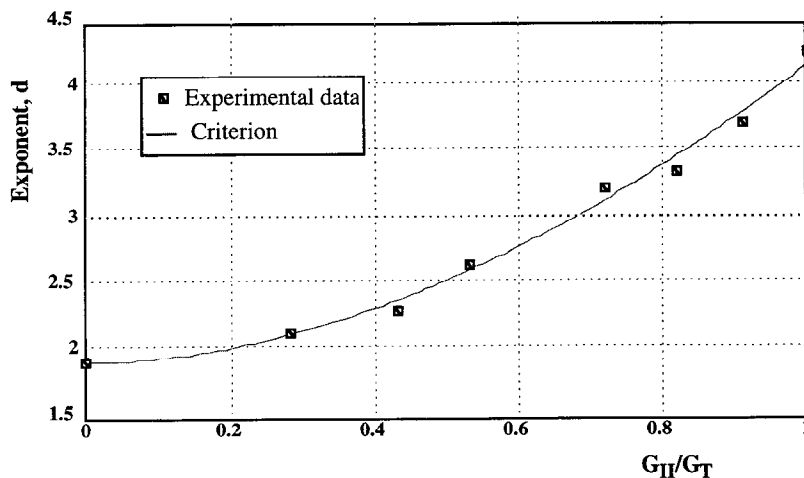


Fig. 14. Exponent d versus $\frac{G_{II}}{G_T}$ mode ratio.

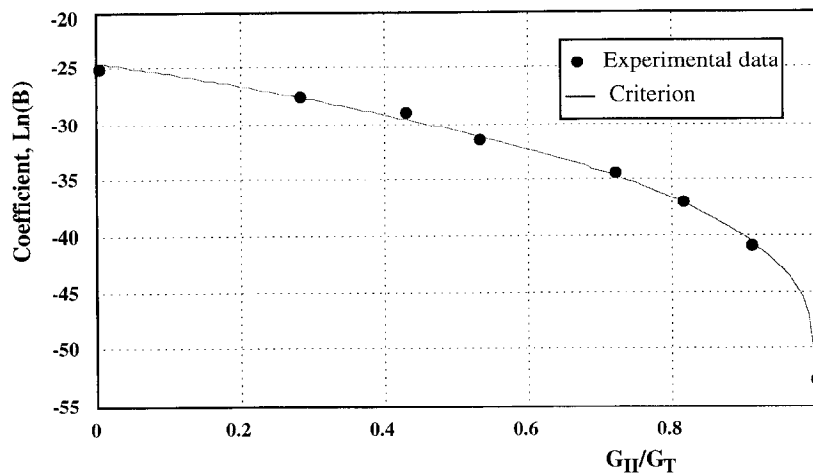


Fig. 15. Coefficient B versus $\frac{G_{II}}{G_T}$ mode ratio.

Table 5. Comparison between results from experiment and criterion

	From experiment	From criterion	Error (%)
d_I	1.9	1.885	0.79
$d_{II} - d_I$	2.34	2.255	3.63
$\ln(B_{II})$	-52.423	-52.616	0.37
$\ln(B_I) - \ln(B_{II})$	27.895	28.058	0.69

6 CONCLUSIONS

The conclusions of this study may be summarised as follows.

1. The MMB apparatus allows characterisation of several cases of mixed-mode delamination under fatigue loading.
2. For each G_{II}/G_T mode ratio considered in this study, results are presented in the form of ΔG_T versus da/dN plots which fit the Paris law.
3. The exponent d and the coefficient B data obey relationships of the form:

$$d = d_I + (d_{II} - d_I) \left(\frac{G_{II}}{G_T} \right)^{m_d}$$

$$\ln(B) = \ln(B_{II}) + [\ln(B_I) - \ln(B_{II})] \left(1 - \frac{G_{II}}{G_T} \right)^{m_B}$$

Good agreement between the experimental results of d and B and the predicted relationships is seen. The exponent d increases as a function of G_{II}/G_T mode ratio with $m_d = 1.85$, whereas the coefficient $\ln(B)$ versus G_{II}/G_T mode ratio decreases with $m_B = 0.35$.

4. The parameters m_d and m_B seem to be characteristic of the material considered.

REFERENCES

1. Crews, J. H. and Reeder, J. R., A mixed mode bending apparatus for delamination testing. NASA TM 100662 Report, National Aeronautics and Space Administration, Washington, DC, 1988.
2. Aboura, Z., Gong, X. J., Sastra, Y. H. and Benzeggagh, M. L., Étude comparative entre deux tests de mode mixte I + II introduisant des géométries d'éprouvettes de types IDCb et MMB. In *Proc. JNC 8*, ed. O. Allix, J. P. Favre and P. Ladevèze, 1992, pp. 679–690.
3. Reeder, J. R. and Crews, J. H., Non linear analysis and redesign of the mixed mode bending delamination test. NASA TM 102777, National Aeronautics and Space Administration, Washington, DC, 1991.
4. Benzeggagh, M. L. and Kenane, M., Mixed mode delamination fracture toughness using MMB apparatus for unidirectional glass/epoxy. *Compos. Sci. Technol.*, 1996, **56**, 439–449.
5. Gong, X. J. and Benzeggagh, M. L., Mixed mode interlaminar fracture toughness of unidirectional glass/epoxy composite. In *ASTM STP 1230*, American Society for Testing and Materials, Philadelphia, PA, 1995, pp. 100–123.
6. Dowling, N. E. and Begly, J. A., Mechanics of crack growth. In *ASTM STP 590*, American Society for Testing and Materials, Philadelphia, PA, 1976, pp. 82–103.
7. Wilkins, D. J., Einsenmann, J. R., Camin, R. A., Margolis, W. S. and Benson, R. A., Characterizing delamination growth in graphite/epoxy damage in composite materials. In *ASTM STP 775*, American Society for Testing and Materials, Philadelphia, PA, 1982, pp. 168–183.
8. Gong, X. J., Rupture interlaminaire en mode mixte I + II du composite stratifié verre/epoxy unidirectionnel et multidirectionnel. PhD thesis, Université de Technologie de Compiègne, 1992.
9. Reeder, J. R. and Crews, J. H., The mixed mode bending method for delamination testing. *AIAA J.*, 1990, **28**, 1270–1276.

10. Russel, A. J. and Street, K. N., The effect of matrix toughness on delamination: static and fatigue fracture under mode II shear loading of graphite fiber composites. In *Toughened Composites*, ASTM STP 937, American Society for Testing and Materials, Philadelphia, PA, 1987, pp. 275–294.
11. Russel, A. J. and Street, K. N., A constant ΔG test for measuring mode I interlaminar fatigue crack growth rates. In *ASTM STP 972*, American Society for Testing and Materials, Philadelphia, PA, 1988, pp. 259–277.
12. Mall, S., Yun, K. T. and Kochhar, N. K., Characterization of matrix toughness effect on cyclic delamination growth in graphite fiber composites. In *ASTM STP 1012*, American Society for Testing and Materials, Philadelphia, PA, 1989, pp. 296–310.
13. Prel, Y., Davies, P., Benzeggagh, M. L. and De Charenteney, F. X., Mode I and mode II delamination of thermosetting and thermoplastic composites. In *ASTM STP 1012*, American Society for Testing and Materials, Philadelphia, PA, 1989, pp. 251–269.
14. Martin, R. H. and Muri, G. B., Characterization of mode I and mode II delamination growth and threshold in AS4/PEEK composite. In *ASTM STP 1059*, American Society for Testing and Materials, Philadelphia, PA, 1990, pp. 251–270.
15. Bathias, C. and Laksimi, A., Delamination threshold and loading effect in fiber glass epoxy composite. In *ASTM STP 876*, American Society for Testing and Materials, Philadelphia, PA, 1985, pp. 217–237.
16. Aboura, Z., Chouchaoui, C. S. and Benzeggagh, M. L., Analytical model of woven composite laminate. Superposition effect of two plies. In *Proc. ECCM 6*, Bordeaux, 1993.
17. Benzeggagh, M. L. and Aboura, Z., Délaminage mode I et II de composites à enfort tissu sollicités à faibles et grandes vitesses. *J. de Phys. III*, 1991, **1**, 1927–1951.
18. Ramkumar, R. L. and Whitcomb, J. D., Characterization of mode I and mixed-mode delamination growth in T300/5208 graphite/epoxy. In *ASTM STP 876*, American Society for Testing and Materials, Philadelphia, PA, 1985, pp. 315–335.
19. Gustafson, C. G. and Hojo, M., Delamination fatigue crack growth in unidirectional graphite/epoxy laminates. *J. Reinf. Plast. Compos.*, 1987, **6**, 36–52.
20. Russel, A. J. and Street, K. N., Predicting interlaminar fatigue crack rates in compressively loaded laminates. In *ASTM STP 1012*, American Society for Testing and Materials, Philadelphia, PA, 1989, pp. 162–178.
21. Dahlen, C. and Springer, G. S., Delamination growth in composite under cyclic loads. *J. Compos. Mater.*, 1994, **28**, 732–781.